Peer-reviewed version available at Geosciences 2018, 8, 8; doi:10.3390/geosciences8010008

Article

Subsidence trends of Volturno River coastal plain (northern Campania, southern Italy) inferred by SAR interferometry data.

Fabio Matano [1,*], Marco Sacchi [1], Marco Vigliotti [2] and Daniela Ruberti [2]

[1] Istituto per l'Ambiente Marino Costiero (IAMC), Consiglio Nazionale delle Ricerche (CNR)
[2] Department of Civil Engineering, Design, Building and Environment (DICDEA), University of Campania "L. Vanvitelli"
* Correspondence: fabio.matano@cnr.it; Tel.: +39-081-542-3834

Abstract: The Volturno Plain is one of the largest alluvial plain of peninsular Italy. This area is characterized by both natural and human induced subsidence, and is and most susceptible to coastal hazards. The present study is based on post-processing, analysis and mapping of the available Persistent Scatterer interferometry datasets, derived from combination of both ascending and descending orbits of three different SAR satellite systems, during an observation period of almost two decades (June 1992 - September 2010). The main output of the research work is a map of the vertical deformation that provides new insights into the areal variability of ground deformation processes (subsidence/uplift) of Volturno plain over the last decades. Vertical displacement values derived by interferometric data post-processing show that the Volturno river plain is characterized by significant subsidence in the central axial sectors and in the river mouth area, whereas moderate uplift is detected in the eastern part of the plain. Other sectors of the study area are characterized by moderate subsidence and/or stability. We infer that the subsidence recorded in the Volturno plain is mainly a consequence of a natural process related to the compaction of the fluvial deposits that fill up the alluvial plain. Anthropic influence (e.g. water exploitation, urbanization) can be substantially regarded as an additional factor that only locally may enhance subsidence. The uplift imaged in the eastern sector of the plain can be related to tectonic activity. The study of subsidence in the Volturno plain is a valuable tool relevant for river flood analyses and coastal inundation hazard assessment addressed to risk mitigation.

Keywords: SAR; alluvial plain; coastal areas; subsidence; Volturno; Italy.

1. Introduction

Most Quaternary alluvial coastal plains of the Mediterranean are affected by significant subsidence due to the simultaneous occurrence of sinking of the ground due to natural and human causes [1, 2, 3, 4] and acceleration of the global sea level rise [5]. Among the main potential drivers of subsidence, there are tectonics [6], compaction of alluvial/coastal plain deposits [7], and fluid extraction [8, 9]. Major effects of subsidence may include inundation of low lands, coastal erosion and aquifer salinization, increased vulnerability to flooding and storm surges, structural damage to infrastructures.

In the last decades, several techniques of satellite-based Synthetic Aperture Radar (SAR) Interferometry (InSAR) have been used to assess ground-surface deformation, related to several dynamic processes, such as subsidence, volcanism, seismicity and tectonics [10, 11, 12, 13, 14, 15, 16]. Two main different approaches have been developed to extract relevant information contained in the phase values of SAR images: Differential SAR Interferometry (DInSAR) and multi-interferograms SAR Interferometry (Persistent Scatterer Interferometry, PSI) techniques [17]. The DInSAR technique depends on the processing of two SAR images of the same target area acquired at different times [18] to detect phase shifts related to surface deformations (i.e. after an earthquake) occurring between the

Peer-reviewed version available at Geosciences 2018, 8, 8; doi:10.3390/geosciences8010008

two reference acquisitions. This approach requires also an external digital elevation model of the analyzed morphological surfaces, from which the topographic phase contribution is estimated and removed from the interferogram. The PSI approach is based on the use of a long series of co-registered, multi-temporal SAR imagery, for which the larger the number of images is, the more precise and robust the results are [17, 19]. The PSI techniques allow producing maps of displacement velocity, measured along the straight line between target and radar sensor (Line Of Sight), and follow the temporal evolution of the displacement at each SAR acquisition epoch.

An overall, retrospective view on the spatial and temporal distribution of ground deformation can be derived for the area of the Campania Region by space-borne multi-temporal DInSAR techniques, based on the analysis of the C-band sensors onboard ERS-1/2, ENVISAT and RADARSAT satellites. A number of Italian national and regional remote sensing projects have recently reported several PSI processed datasets referred to Campania territory [20, 21, 22, 23, 24, 25, 26]. The various datasets have been acquired as the result of implementation of different processing techniques, such as Permanent Scatterers (PS-InSAR) [27], Persistent Scatterers Pairs (PSP) [19, 28, 29] and Small BAseline Subset (SBAS) [30, 31, 32]. Integrated results from these techniques may provide very accurate displacement measurements along SAR Line Of Sight (LOS), which yield accuracy in the order of millimeters [27, 28, 29, 30, 31, 32, 33].

The use of SAR interferometry measurements to accurately analyze ground subsidence and/or uplift processes of different origin has been already tested and validated in several sectors of Campania Region [16, 33, 34, 35, 36, 37, 38]. In this research we use PS-InSAR and PSP datasets, both relying on the analysis of pixels which remain coherent over a sequence of interferograms (PSI techniques), as they are available for the entire study area over a relatively long time period (1992-2010).

The aim of the present study is the quantitative analysis of the ground deformation trends referred to about two decades (1992-2010), which characterize the alluvial plain of the Volturno River, located in northern sector of Campania (Italy) (Fig. 1).

The research work was based on post-processing, mapping and interpretation of available ground deformation datasets [13, 20, 21, 22, 23, 24], obtained from interferometric processing with PS-InSAR and PSP techniques of ERS-1/2 (1992-2001), RADARSAT (2003-2007) and ENVISAT (2003-2010) radar satellite scenes, provided by European Space Agency (ESA).

The Volturno plain has been largely investigated in recent years as a representative case of the main land-use and hydro-geomorphological changes characterizing the urbanized coastal plains of the Mediterranean Sea during the last half century. Environmental changes documented for the Volturno coastal plain include dramatic alteration of alluvial channels, floodplain and the deltaic environment, as well as coastline retreat [37, 39, 40, 41, 42]. Previous studies have suggested that the considerable subsidence affecting the Volturno plain area may be interpreted as the result of a negative balance between the groundwater recharge of the Volturno alluvial plain and the water drainage by the channel system realized for industrial purpose and intense agricultural activity [16, 43]. Based on GIS overlay, Riccio [44] has pointed out, however, that there is no spatial correlation in the Volturno plain between subsidence rates and the agricultural land use and/or livestock farming and cattle breeding areas. Aucelli et al. [37] elaborated risk inundation maps for the coastal area of the plain by comparing sea level rise forecasts and subsidence trends.

Our study presents a new quantitative scenario for ground deformation in the Volturno plain following the method developed by Vilardo et al. [16]. Previous studies [16, 37] have referred only to ERS-1/2 dataset, related to the time interval 1992-2000. The main purpose of this research was to obtain a map of cumulated ground deformation for the study area over the period 1992-2010, relying on three different SAR datasets, provided by various satellites. The outcomes of our analysis are also discussed on the basis of the geological setting of Volturno Plain and subsurface stratigraphic data.

2. Geological, geomorphological and land use framework

The Campania Plain is part of a large extensional sedimentary basin mostly formed during the Quaternary between the western flank of the southern Apennines and the eastern Tyrrhenian margin

Preprints (www.preprints.org) | NOT PEER-REVIEWED | Posted: 16 November 2017 doi:10.20944/preprints201711.0112.v1

Peer-reviewed version available at Geosciences 2018, 8, 8; doi:10.3390/geosciences8010008

[45, 46, 47, 48, 49, 50]. The plain is surrounded by calcareous-dolomitic mountain ridges (Fig. 1), delimited by NW-SE trending regional normal faults, whereas its carbonatic and volcanic substratum is affected by extensional tectonics with NE-SW, NW-SE and E-W trending faults [51, 52, 53, 54, 55]. Some of these lineaments correspond to normal faults that have been active since the Late Pleistocene and display vertical slip rate in the order of 0.2 - 2.5 mm/yr [51].

The area was largely submerged by the sea water since mid-late Pleistocene, when extensional tectonics accompanied by the onset of an intense volcanic activity, locally developed across the continental margin [56]. At ca. 39 ky BP, a highly explosive eruption covered the entire Campania Plain with an ignimbrite deposit, up to 55 m thick, known as Campanian Ignimbrite or Grey Tuff (CGT) [57, 58, 59, 60]. This unit represents the substrate for the uppermost Pleistocene-Holocene and recent sedimentation. A subsequent eruption, dated at ca. 15 ky BP [61], led to deposition of another ignimbrite deposit, the Neapolitan Yellow Tuff (NYT), which is primarily exposed in the urban area of Naples and at the Campi Flegrei (or Phlegrean Fields area). Tuff units (CGT and NYT) and related ash deposits include most of the Quaternary volcaniclastic products cropping out in the Campania Plain (Fig. 1).

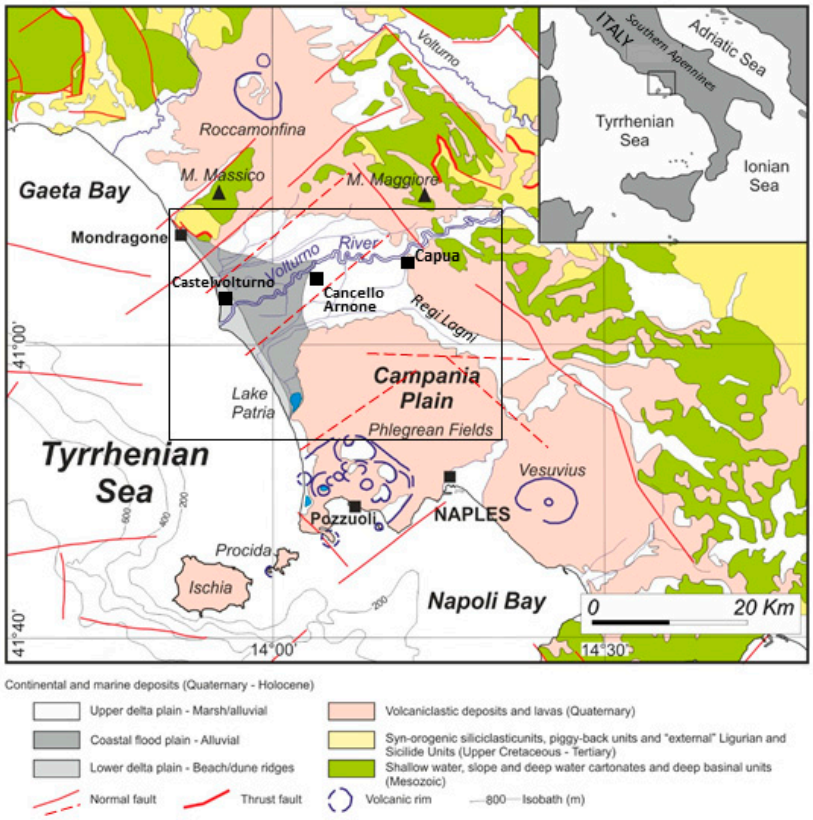

Figure 1. Geological map of the Campania Plain. Black frame indicates the study area.

The latest Pleistocene-early Holocene (ca. 16 ky – 6 ky BP) sea-level rise caused a rapid flooding of the lower paleo-Volturno incised valley, accompanied by the formation of a pronounced embayment at the mouth of paleo Volturno estuary and a landward widening of the continental shelf. Since ca. 6.5 ky BP a coastal progradational phase was established, allowing for the onset of the present-day alluvial plain. The coastal area evolved as a wave-dominated delta system, with flanking strandplains forming beach-dune ridges partially enclosing lagoon-marshy areas [62, 63] (Figs. 1 and 2). Beach and lagoon environments persisted up to 2 ky BP. Since then, crevasse splay and overbank deposits filled most of the swamp areas. Evidence for a persisting progradational trend of the shoreline is documented since the 3rd century BC [39, 64]. During the last century, a significant

shoreline retreat, related to the decrease in river sediment load, affected the Volturno River mouth, particularly at the delta cusp [39, 41, 65].

The studied sector of the Volturno plain is characterized by a flat morphology (Fig. 3), with slope lower than 5° and elevation ranging between 0 and 40 m a.s.l. from the coastline to the north of Capua. The plain is bordered seaward by a 40 km long sandy beach, behind which a wide lowland area with an elevation between 0 and – 2 m a.s.l. is present (Fig. 3). This area is regarded as the remnant of an ancient barrier lagoon system [62, 66, 67, 68], and is characterized by clayey and silty alluvial deposits (Fig. 2) locally interbedded with peat layers [42].

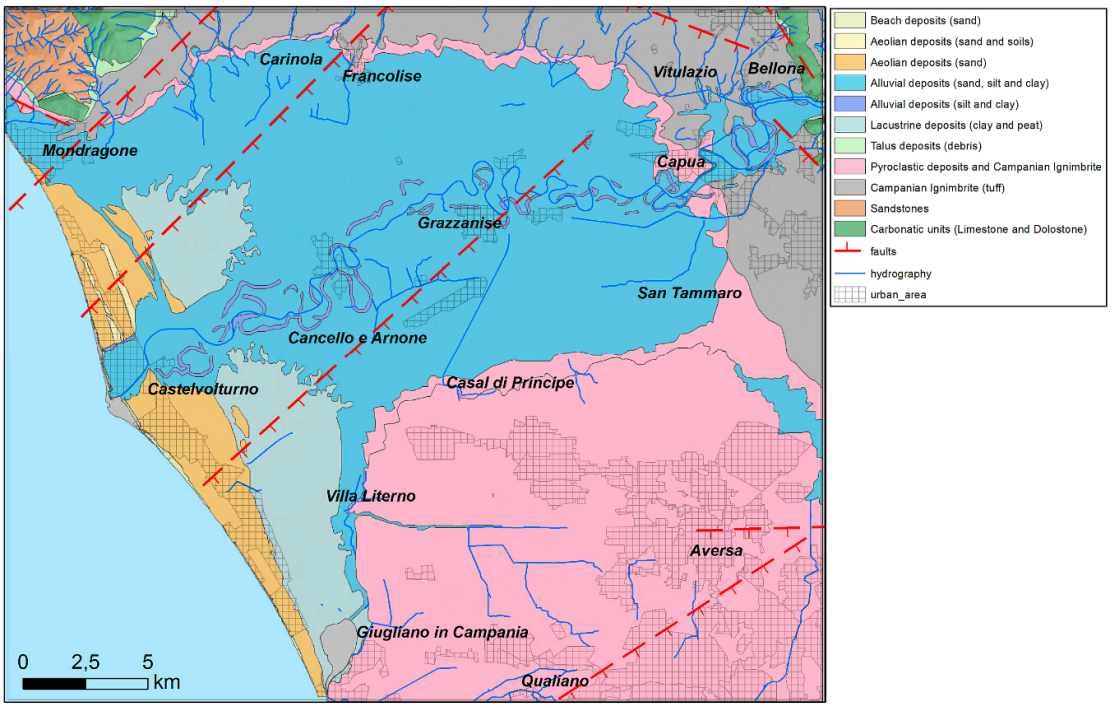

Figure 2. Geological map of the Volturno Plain (based on Geological Map of Italy and stratigraphic data [62, 63, 70]).

Most of the coastal plain marshy areas were reclaimed since the XVI century, allowing for the development of agriculture and farming, but also severe urbanization along the coastal zone, at the expenses of the beach-dune system, and along the river course, since the mid-1900s [42]. Human activity often resulted in dramatic changes of the landscape, loss of coastal wetland and accelerated coastal erosion [39, 40, 41, 65]. The effects of the above anthropic impacts are nowadays adding complexity to a scenario characterized by long-term land subsidence and a predicted sea-level rise [69].

The study area is incised by a network of natural and artificial streams, belonging to two major hydrographic catchments, namely related to the Volturno River and Regi Lagni channel. The relatively flat morphology of coastal plain is characterized by the occurrence of a topographic high (up to 8-10 m a.s.l.) formed by Holocene dune ridge, that develops in NW-SE direction at ca 4 km inland with respect to the present-day current shoreline. The ridge is locally interrupted by the linear erosion associated with the course of the Volturno River, Regi Lagni channel and Patria Lake emissary [37].

The Volturno plain is characterized by a locally high concentration of infrastructure (roads, railways, etc.) and inhabited areas, both in coastal sectors (Castelvolturno and Mondragone towns) and in inland areas (Capua, Cancello Arnone), where also several farming, agricultural and cheese production activities are located.

Land use shows a strong agricultural activity in the Volturno plain, and indicates that fields are almost all (81,1 %) farmed both in summer and in winter season. The urbanized environment

Preprints (www.preprints.org) | NOT PEER-REVIEWED | Posted: 16 November 2017 doi:10.20944/preprints201711.0112.v1

Peer-reviewed version available at Geosciences 2018, 8, 8; doi:10.3390/geosciences8010008

represents a relevant percentage of the area (7,4 %), and it extends mainly along the coast. Grain cereals and grass cultivations are prevailing, mostly in association to numerous zootechnical activities of the area. Most of them are buffalo farming companies. Both cattle breeding and agricultural activities require high amount of water.

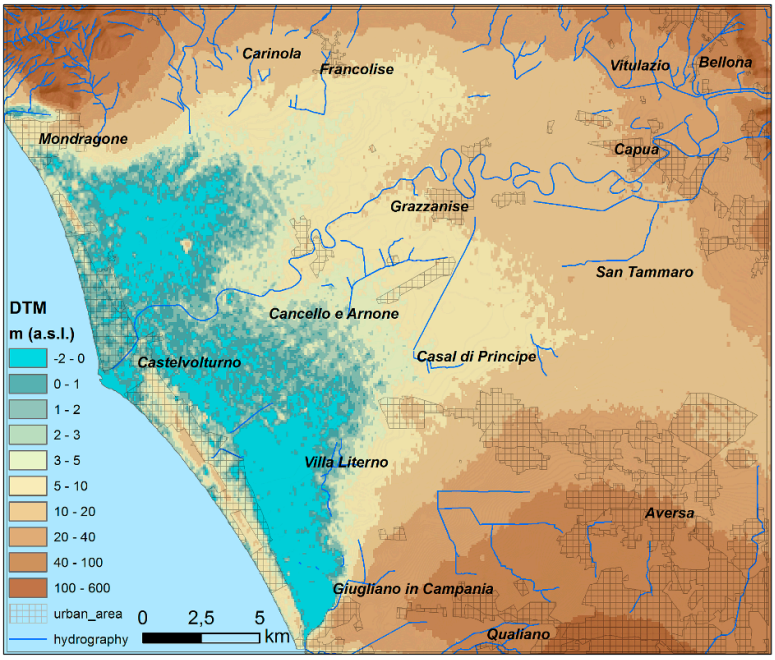

Figura 3 – Altimetry classes of the Volturno Plain from DTM with 70 m cell size.

3. Materials and Methods

Several interferometrically processed (PSI approach) datasets, derived by some Italian national [23, 24, 25] and Campania regional [13, 20, 21, 22] remote sensing projects, are available for research activity and territorial planning and monitoring.

Recent trends in ground deformations for the Italian territory have been made available by processed sets of archive SAR images of ERS-1/2, RADARSAT 1 and ENVISAT satellites. The interferometric processing was performed both at national scale, within the frame of the Not-Ordinary Plan of Environmental Remote Sensing [23, 24] by means of the Persistent Scatterer Pair (PSP) technique [19, 28, 29], and at a regional scale, within the activities of the TELLUS Project [13, 20, 21, 22] by means of the Permanent Scatterers (PS-InSAR) standard technique [27].

The PS-InSAR processing allows for detecting the displacements through time of man-made or natural reflectors (Permanent Scatterers, PS), along the radar LOS. This is obtained, by separating time-dependent surface motions, atmospheric delays, and elevation-error components of the measurement [27, 71, 72, 73]. The main results for each PS consist of a time series of the variation in the sensor-target distance along the LOS (ground deformation) over the entire acquisition period, and include the annual average velocity of the displacement calculated by linear fitting. This technique requires a master scene and a stable reference point, assumed motionless, to which the zero in the time series and the relative measurements of deformation are respectively referred [27].

The PSP technique [19, 28, 29] overcomes some limitations of other PS standard methods. Thanks to the pair-of-point approach, the PSP outputs are not affected by artifacts slowly variable in space, like those depending on atmosphere or orbits, and guarantees very dense and accurate displacement measurements, both for anthropic structures and natural terrains [19].

The ERS-1/2, RADARSAT and ENVISAT satellites provided a comprehensive archive of imagery, which is currently used as a retrospective tool for historical interferometric monitoring of ground deformations. With reference to the Volturno plain study area that extends for about 770 km^2,

354 images of ERS-1/2, RADARSAT 1 and ENVISAT satellite were used for PSI interferometric processing in the source projects (Table 1).

The average incidence angles of LOS range from 22° to 34°, with a relevant difference between ERS-1/2 - ENVISAT (22° to 25°) and RADARSAT (32° to 34°) angles (Table 1). The ERS-1/2 reference time range is from June 1992 to December 2001, whereas ENVISAT and RADARSAT acquisition period ranges from November 2002 to July 2010 with overlapping datasets between March 2003 and September 2007 (Table 1).

For the study area we have collected and post-processed six PS datasets (Table 2): a) ENVISAT ascending orbit, b) ENVISAT descending orbit, c) RADARSAT ascending orbit, d) RADARSAT descending orbit, e) ERS-1/2 ascending orbit, f) ERS-1/2 ascending orbit. The PS datasets include about 506.000 PSs, identified within the study area with coherence higher than 0.65. The selected datasets are characterized by negative mean values of displacement velocities in both ascending and descending orbits (Table 2). Specific PSI techniques used for each dataset are also listed (Tab. 2).

Table 1. Orbital parameters of interferometrically processed [20, 21, 22, 23, 24, 25] satellite images.

Satellite - Orbit	Track / Frame	LOS incidence angle	Used scenes	Time range
ENVISAT – Descending	36 / 2781	22°	41	05 Jun. 2003 – 03 Jun. 2010
ENVISAT – Ascending	358, 129 / 819	25°	60	13 Nov. 2002 – 30 Jul. 2010
RADARSAT - Ascending	104 / S3	34°	52	4 March 2003 –15 Sept. 2007
RADARSAT - Descending	11, 111 / S3	32-33°	51	5 March 2003 –23 Aug. 2007
ERS-1/2 - Ascending	129 / 801	22°	69	14 Jun 1992 – 13 Dec 2000
ERS-1/2 - Descending	36, 265 / 2781, 2783	23°	81	8 Jun. 1992 – 23 Dec. 2001

PS datasets have been georeferenced to projection WGS-84 UTM Zone 33N, and spatially processed using GIS software. Each point of the four PS shapefile datasets is identified by coordinates (North, East) and a set of attributes, including: a) identifier code; b) average velocity of entire acquisition time period, expressed in mm year^{-1}; c) standard deviation of the average velocity; d) coherence; e) a subset of measurements, expressed in mm, of the displacement along the LOS of each PS. The PS coherence is a normalized index of the local signal-to-noise ratio of the interferometric phase and reflects the accuracy of PS measurements [14, 74, 75, 76]. The PSI processing allows obtaining very accurate measurements within 1.0 mm/year for the PS average velocity along the LOS by assuming a threshold value of 0.65 for coherence [33, 71, 75, 77, 78] thanks to the large number of SAR images used for the processing (Table 1).

Due to the side-looking view of SAR satellite sensors, PS displacements are measured along the LOS, which ranges from 22° to 34° in the study area (Table 1). The availability of both ascending and descending datasets allowed for the evaluation of the vertical components of the deformation for the

Preprints (www.preprints.org) | NOT PEER-REVIEWED | Posted: 16 November 2017 doi:10.20944/preprints201711.0112.v1

Peer-reviewed version available at Geosciences 2018, 8, 8; doi:10.3390/geosciences8010008

areas in common with both the acquisition geometries, based on simple trigonometric calculations [16, 33]. We could extract only two spatial components of ground deformation (vertical and E-W horizontal components), as the N-S horizontal component cannot be valued by the SAR satellite acquisition system [16].

The mean displacement rates were used to derive the annual average ground deformation LOS velocity maps for ascending and descending orbits of ERS-1/2, RADARSAT and ENVISAT PS data by Inverse Distance interpolation Weighted (IDW) method. IDW approach is commonly used to interpolate scattered points, thus allowing preservation of local variability of the data and suitable results [37, 79, 80]. An interpolation method, consisting in a quadratic weighting power 2 within a 500 m radius neighborhood [16, 33], was used to obtain 50 m regularly spaced grids. The vertical components of the mean annual velocity of the ground deformation were computed, using the ascending and descending LOS velocities ($vLOS_{asc}$ and $vLOS_{desc}$) raster maps derived from ERS-1/2, RADARSAT and ENVISAT data.

Table 2. Summary of PS datasets used in this study.

Satellite - Orbit	PSI technique	count	PS velocity - mean (mm/yr)	PS stand. dev. - mean	PS coherence - mean	PS density (num./km²)
ENVISAT - Ascending	PSP	105.319	- 0.88	0.31	0.73	136.8
ENVISAT - Descending	PSP	120.557	- 0.40	0.39	0.77	156.6
RADARSAT - Ascending	PS-InSAR	57.563	- 1.32	1.31	0.84	74.8
RADARSAT - Descending	PS-InSAR	55.324	- 0.96	0.72	0.85	71.8
ERS-1/2 - Ascending	PSP	73.694	- 1.08	0.73	0.73	95.7
ERS-1/2 - Descending	PSP	93.480	- 0.80	0.50	0.68	121.4

The vertical component of the velocity was calculated by combining the $vLOS_{asc}$ and $vLOS_{desc}$ raster maps on pixels common to both maps [13, 16, 32, 33, 81, 82], assuming that the ascending and descending LOS belong to the East-Z plane and the look-angle is the same for both ascending and descending geometries. Based on these assumptions, we use equation (1) [16, 33]:

$$vVert = \frac{(vLOSdesc + vLOSasc)/2}{\cos(q)} \quad (1)$$

where "v" is the displacement velocity vector of an investigated PS, vVert is the projection along the Cartesian vertical axes, vLOSdesc and vLOSasc are the projections of velocity along different LOSs, and q is the look-angle. For the calculation of vVert related to each satellite dataset we used a value of q given by the average of the two LOS incidence angles of the ascending and descending orbits: i.e. 22.5° for ERS-1/2, 33.25° for RADARSAT and 23.5° for ENVISAT. The obtained 50 m spaced grid maps show the distribution of the vertical components of ground deformation velocity in the

Volturno Plain for the datasets 1992-2000 (ERS-1/2), 2003-2007 (RADARSAT) and 2003-2010 (ENVISAT).

In order to obtain a quantitative assessment of the subsidence process, we have calculated the amount of vertical ground deformation based on the average yearly vertical velocity for each satellite datasets and the number of years of the time interval to which they are referred (i.e. 9 years for ERS-1/2, 2.5 years for RADARSAT and 5.5 years for ENVISAT, as the overlapping years of RADARSAT and ENVISAT datasets count 0.5 year each). The result is a 50 m spaced grids map, showing the cumulated distribution of vertical movements in the Volturno Plain, expressed in millimeters, for the period 1992-2010.

4. Results

4.1. LOS velocity fields

The LOS velocity data distribution obtained by the post-processing of PS datasets is mainly characterized by negative values in both ascending and descending orbits for all satellite datasets (Table 3). The mean and median LOS velocity values are negative (respectively ranging from – 1.32 to – 0.40 mm/yr and from – 0.83 to – 0.01 mm/yr) for all datasets, showing an asymmetrical distribution toward negative values, due to the general subsidence affecting the plain (skewness ranging from -3.62 to – 1.49). The Quartile (Q1, Q3) values and the interquartile range (IQR) are similar for all datasets (Table 3). The ranges of "normal" values (less and more than two standard deviations away from the mean), that account for ca. 95% of all data, show very similar values for all datasets (Table 3). This implies that the distribution of the most part (95%) of the data in all datasets is homogenous, and describe a constant and persistent process of ground deformation at regional scale. Only the extreme maximum and minimum values of velocity (representing ca. 5% of all data) show significant differences, that are usually due to very local causes (e.g. instabilities of anthropic structures or buildings, water extraction from the subsurface or infiltration).

Table 3. Data distribution statistics of LOS velocity data in the used datasets.

Satellite - Orbit	mean	std. dev.	skewness	Q1	median	Q3	IQR	-2 s.d.	+2 s.d.	min	max
ENVISAT - Ascending	- 0.88	2.14	-3.32	-1.20	-0.20	+0.30	1.50	- 5.16	+ 3.40	- 31.30	+ 7.80
ENVISAT - Descending	- 0.40	1.88	-3.16	-0.80	-0.01	+0.60	1.40	-4.16	+3.36	- 28.10	+ 5.70
RADARSAT - Ascending	- 1.32	2.60	-1.49	-2.25	-0.83	+0.10	2.35	-6.52	+3.88	- 34.25	+ 26.09
RADARSAT - Descending	- 0.96	2.45	-2.52	-1.49	-0.57	+0.21	1.70	-5.86	+3.94	- 35.02	+ 16.51
ERS-1/2 - Ascending	- 1.08	2.41	-3.62	-1.26	-0.46	+0.08	1.34	-5.90	+3.74	- 38.87	+ 8.26
ERS-1/2 - Descending	- 0.80	2.23	-3.47	-1.05	-0.26	+0.31	1.36	-5.26	+3.66	- 37.22	+ 6.71

Preprints (www.preprints.org) | NOT PEER-REVIEWED | Posted: 16 November 2017 doi:10.20944/preprints201711.0112.v1

Peer-reviewed version available at Geosciences 2018, 8, 8; doi:10.3390/geosciences8010008

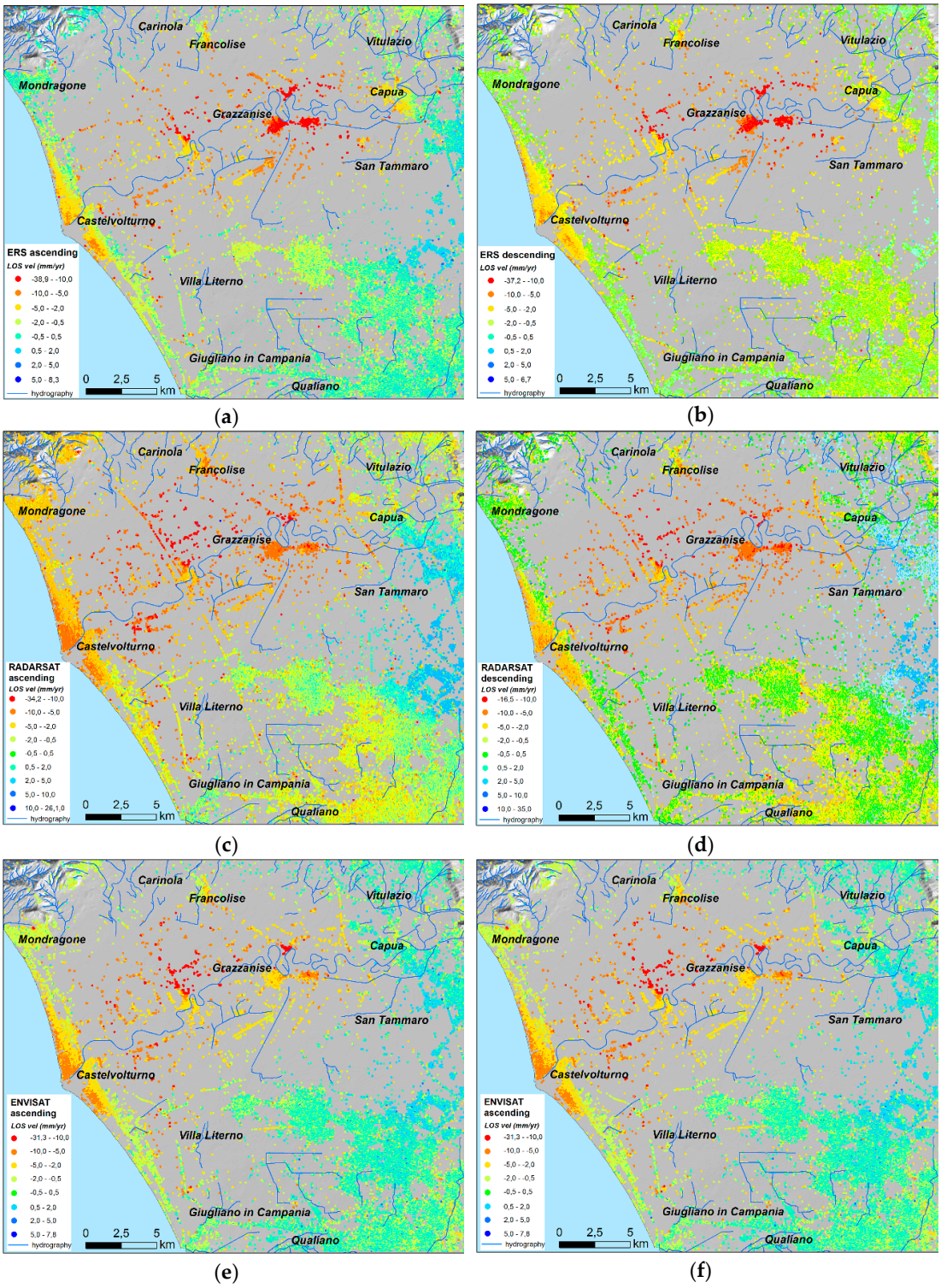

Figure 4. Map view of range-change rate measurements (LOS velocity) of PS with coherence ≥0.65 of the six used datasets: (a) ERS-1/2 ascending orbit; (b) ERS-1/2 descending orbit; (c) RADARSAT ascending orbit; (d) RADARSAT descending orbit; (e) ENVISAT ascending orbit; (f) ENVISAT descending orbit.

The spatial distribution of PS yearly average LOS velocity values is showed in different maps for both ascending and descending orbits of ERS-1/2, RADARSAT and ENVISAT datasets (Fig. 4), that show a similar geographical distribution of PSs. Most of the PS are concentrated along linear

infrastructures (roads, railway, etc.) and over urban areas, where the concentration of buildings and other manufactured structures is very high (Fig. 4). Even if areas of no data may locally occur, the overall distribution of PS is sufficiently homogenous for a regional analysis of ground deformation. If we consider the PS density (Table 2), we may observe that ERS-1/2 and ENVISAT datasets are characterized by higher values, comprised between 96 and 157 PS/km^2, whereas RADARSAT datasets are characterized by lower values of PS density (72 to 75 PS/km^2). This difference depends on the adopted procedure, as the PSP technique, used for ERS-1/2 and ENVISAT data processing, results in a denser distribution of points for the measurement of displacement [19].

The spatial distribution of the mapped velocity classes display a common general trend in the six datasets, even though some differences can be recognized in the different maps (Fig. 4). The lowest LOS velocity values (lower than -10 mm/yr) are recorded in the central sector of the study area (around Grazzanise) and along the Volturno River (Fig. 4). The Volturno river mouth shows moderate negative LOS velocity values (-2 to – 10 mm/yr), whereas positive values (+ 2 to + 10 mm/yr) are recorded in the eastern sector (eastward Capua and San Tammaro cities).

More in detail, RADARSAT and ENVISAT datasets display higher positive values in the eastern sector of the study area and less negative values in the central sector of the study area if compared with ERS-1/2 datasets, showing some changes in the intensity of subsidence/uplift velocity during the two decades of observation. Moreover, some datasets shows differences in the displacement rates obtained from ascending and descending geometries.

RADARSAT datasets show some differences along the coastal area, near Castelvolturno, which display higher subsidence in ascending datasets. RADARSAT and ERS datasets are characterized by lower positive values in descending datasets in the eastern uplifting sector. Along the southern sector of the study area, minor differences can be found between ascending and descending RADARSAT and ERS datasets. These differences can be related to non-vertical movements affecting those sectors like, for example, local displacement from East to West along the horizontal component of ground deformation for the coastal area and the eastern sectors.

It is to be noted that the difference between LOS angles characterizing the two orbital systems (32-34° vs. 22-25°) (Tab. 1) can only justify a difference of few mm/yr in the values of LOS velocity referred to the same ground deformation phenomenon. Consequently only a minor part of the discrepancy between RADARSAT AND ERS/ENVISAT datasets can be ascribed to the geometrical differences in the satellite acquisition geometry.

4.2. Vertical components of ground deformation velocity

The maps of the vertical component of the displacement velocity, derived by the processing of ascending and descending LOS velocities maps, shows that the study area has been characterized by similar vertical velocity patterns over the periods 1992-2000 (Fig. 5a), 2003 - 2007 (Fig. 5b) and 2003-2010 (Fig. 5c) time intervals.

All the vertical velocity maps (Fig. 5) indicate significant ground deformation in central-northern part of the Campania plain, mostly concentrated along course of Volturno River and around Grazzanise, with subsidence rates in the order of −33 to −15 mm/year, at least since the early 90's. Wider areas, also affected by significant subsidence processes with rates of −15 to −5 mm/year, may be found along the Volturno river channels in the central sector of the plain and along the lateral flood plains, on the lowland area at the back of the dune system (Villa Literno) and at the estuary area of Castelvolturno. An uplift sector with positive (uplift) rates of +0.25 to + 8 mm/year is detected to the East of San Tammaro, in the eastern sector of the study area.

Even though the main ground deformation trends are consistent throughout the processed datasets, the differences between subsiding and uplifting sectors appear more marked and extended on the 2003-2010 maps (Fig. 5b-c), which show uplifting sectors displaying rates up to + 8 mm/yr. Subsiding areas of intermediate class (- 5 to -10 mm/yr), instead, appear wider on the 2003-2007 map (Fig. 5b).

Preprints (www.preprints.org) | NOT PEER-REVIEWED | Posted: 16 November 2017 doi:10.20944/preprints201711.0112.v1

Peer-reviewed version available at Geosciences 2018, 8, 8; doi:10.3390/geosciences8010008

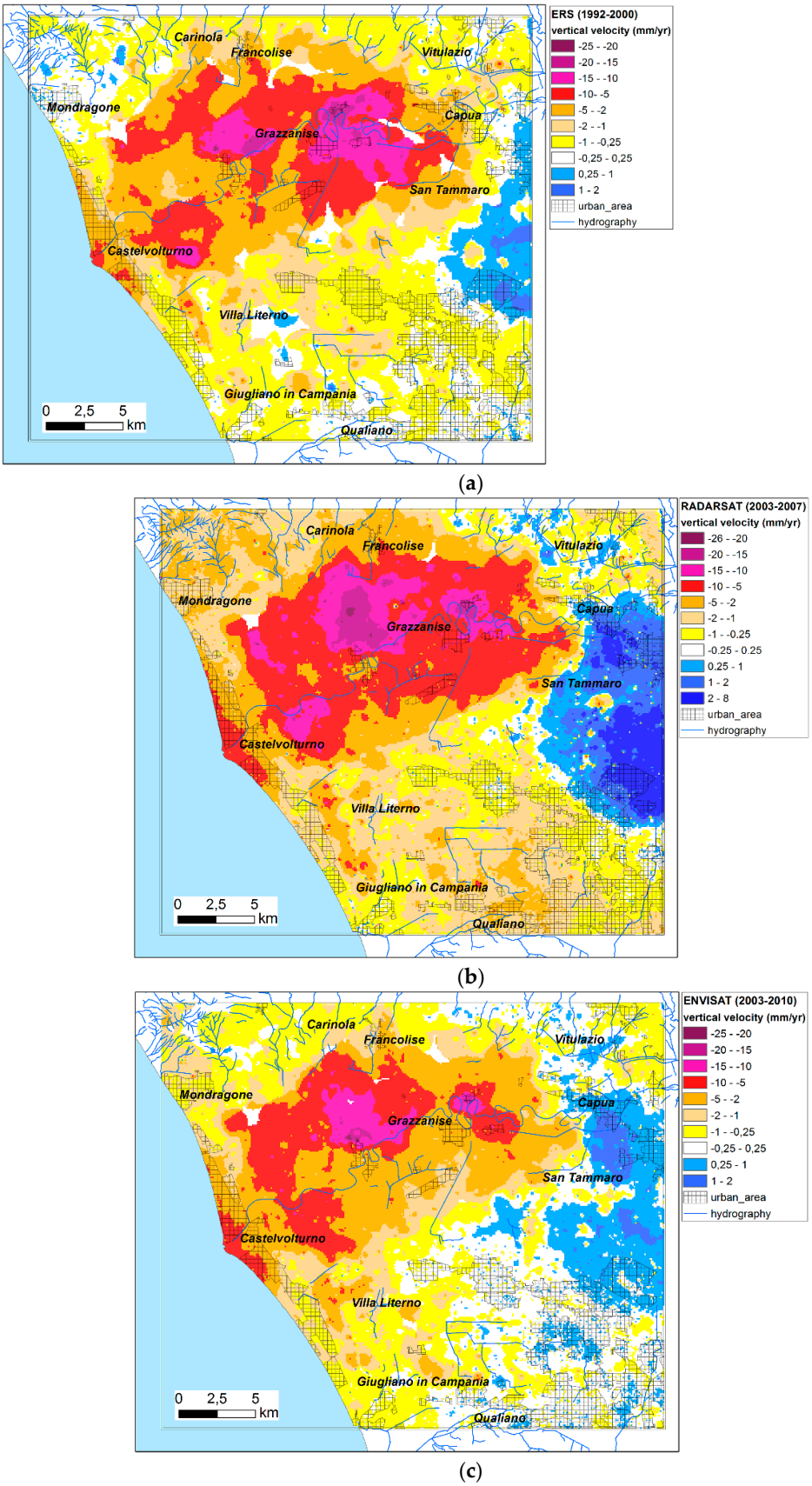

325 **Figure 5.** Vertical components of ground deformation velocity detected by interferometric processing
326 of ERS-1/2 (**a**), RADARSAT (**b**) and ENVISAT (c) datasets.

Preprints (www.preprints.org) | NOT PEER-REVIEWED | Posted: 16 November 2017 doi:10.20944/preprints201711.0112.v1

Peer-reviewed version available at Geosciences 2018, 8, 8; doi:10.3390/geosciences8010008

When considering the differences in vertical velocity rates between RADARSAT and ENVISAT datasets in the uplifting sector (Fig. 6), it can be seen that they are mainly limited to 1-3 mm/yr, with RADARSAT velocity rates higher than in the case of the ENVISAT datasets. These differences, likely depending on the different values of LOS incidence angle of the two orbital systems, may actually reflect a net change in the intensity of subsidence/uplift velocity between the two periods. The same considerations can be made for areas affected by subsidence, characterized by different negative values in RADARSAT and ENVISAT datasets.

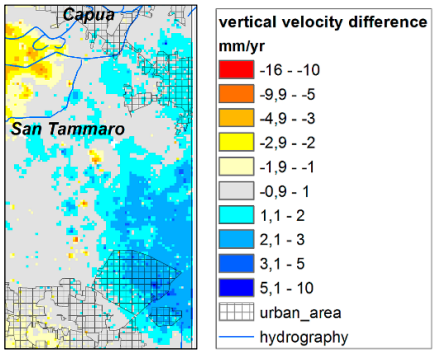

Figure 6. Differences in vertical velocity ranges between 2003-2007 RADARSAT and 2003-2010 ENVISAT datasets in the uplifting eastern sector of the study area.

4.3. Subsidence assessment

A quantitative assessment (expressed in mm) of subsidence and uplift processes affecting the Volturno plain has been obtained by calculating the cumulate amount of the vertical deformation of ground surface derived by the average annual vertical velocity of the three processed satellite datasets. The map of Fig. 7 shows that ca. 89% of the study area (685 km²) is characterized by negative values (from 0 to – 417.4 mm) and only the remaining part, representing ca. 11% of the area (85 km²) is characterized by positive values (from 0 to + 40 mm) in the analyzed time interval (1992-2010).

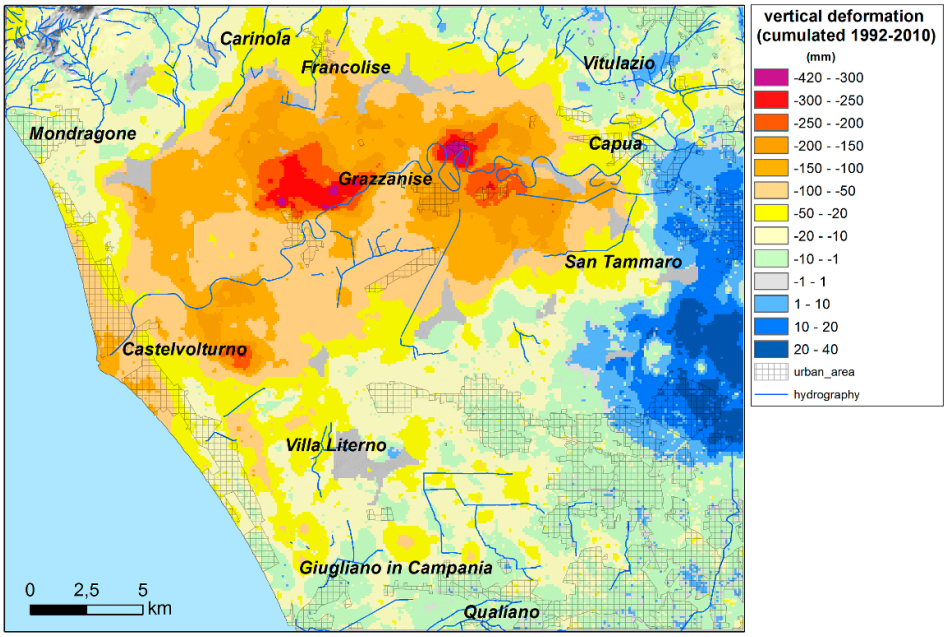

Figure 7. Cumulated amount of vertical ground displacement estimated during 1992-2010.

If we regard as stable the coastal plain sectors characterized by vertical ground movements with values between +10 and – 10 mm (green, gray and light blue colors in the map of Fig. 7), we may define a number of areas with a total extension of ca. 200 km² (26% of the study area), showing no significant evidence of subsidence or uplift during the period 1992-2010 . Conversely, the central part of the Volturno Plain shows a large area of 215 km², corresponding to ca. 30% of the investigated area, that displays subsidence values ranging from - 50 to - 418 mm. This sector is characterized by a complex deformation pattern (Fig. 7) with the highest negative values (lower than - 200 mm) along the course of the Volturno River between the cities of Cancello Arnone and Grazzanise. High subsidence values (- 50 to - 200 mm) are found in the more external sectors of the alluvial plain, and in the back-dune depressions, that extend for ca. 8 km², in the vicinity of Villa Literno. The coastal sector close to the Volturno river mouth (ca. 10 km²), is characterized by moderate subsidence values (- 50 to - 150 mm), whereas the dune ridge system shows very slight subsidence or stability. Low subsidence (- 10 to - 50 mm) also characterize the remaining sectors of the plain, to the North and to the South of the Volturno River. The eastern sector (East of San Tammaro and Capua cities), extending for ca. 40 km² and corresponding to ca. 5% of the investigated area, displays moderate uplift with vertical ground movements between +10 mm and + 40 mm (Fig. 7).

5. Discussion

Vertical deformation values derived by post-processing of PSI datasets utilized in this study indicate that the Volturno river plain is characterized by a complex trend of vertical ground deformation during 19 years of observation (1992-2010). A moderate subsidence (between - 50 mm and – 10 mm) has characterized most of the investigated area. Severe subsidence has been detected in the central sectors of the plain, with ground deformation lower than - 200 mm along the course of the Volturno River, and values lower than - 150 mm close to the river mouth. Conversely, the eastern part of the study area, East of San Tammaro and Capua is characterized by the occurrence of a slightly uplifting sector (Fig. 7).The maps realized in this study, based on results deriving from different datasets (Fig. 5), indicate that the study area is generally characterized by consistent vertical velocity patterns during the two periods of observation (1992-2000 and 2003-2010). LOS displacement time series (Fig. 8) of some exemplificative PS located (Fig. 9) both in subsiding sector, near Grazzanise, and in uplifting sector, near San Tammaro, display mainly linear trends, characterized by continuous subsidence or uplift with similar rates through time. This behavior is substantially different from the one that is observed in adjacent structural domain of the Campi Flegrei (Fig. 1). In fact, LOS displacement time series (Fig. 8b) derived from selected PS located near Pozzuoli, clearly indicate that the Campi Flegrei district is characterized by remarkably non-linear behavior of ground deformation, due to repeated alternation between phases of uplift and subsidence, ostensibly related with active volcano-tectonic processes occurring in the volcanic caldera [12].

The interpretation of mechanisms controlling ground deformation patterns in the Volturno Plain is quite complex, as the entire coastal area has suffered from severe land use and profound landscape modifications during the last three centuries [42]. On the coastal zone, especially along the shoreline [37, 42], a wild growth of both touristic and residential housing over the last decades has resulted in a dramatic environmental impact. The increasing construction load and water pumping activity have in fact contributed, in turn, to enhance the longer-term subsidence rates due to tectonics [47, 48], as suggested by a comparison of the 1992-2000 ERS-1/2 with the dataset (Fig. 4a) to 2003-2010 RADARSAT - ENVISAT datasets (Fig. 4b-c).

Vilardo et al. [16] have proposed that the subsidence characterizing the Volturno plain is mostly due to the negative balance between the water recharge rates of the Volturno basin and the drainage operated by the artificial channeling related to industrial and intense agricultural activities. The lack of unequivocal correlation between subsidence trends and agricultural land use and zootechnical farms location [44] seems to indicate that these human activities do not exert significant impact on regional subsidence rates.

Preprints (www.preprints.org) | NOT PEER-REVIEWED | Posted: 16 November 2017 doi:10.20944/preprints201711.0112.v1

Peer-reviewed version available at Geosciences 2018, 8, 8; doi:10.3390/geosciences8010008

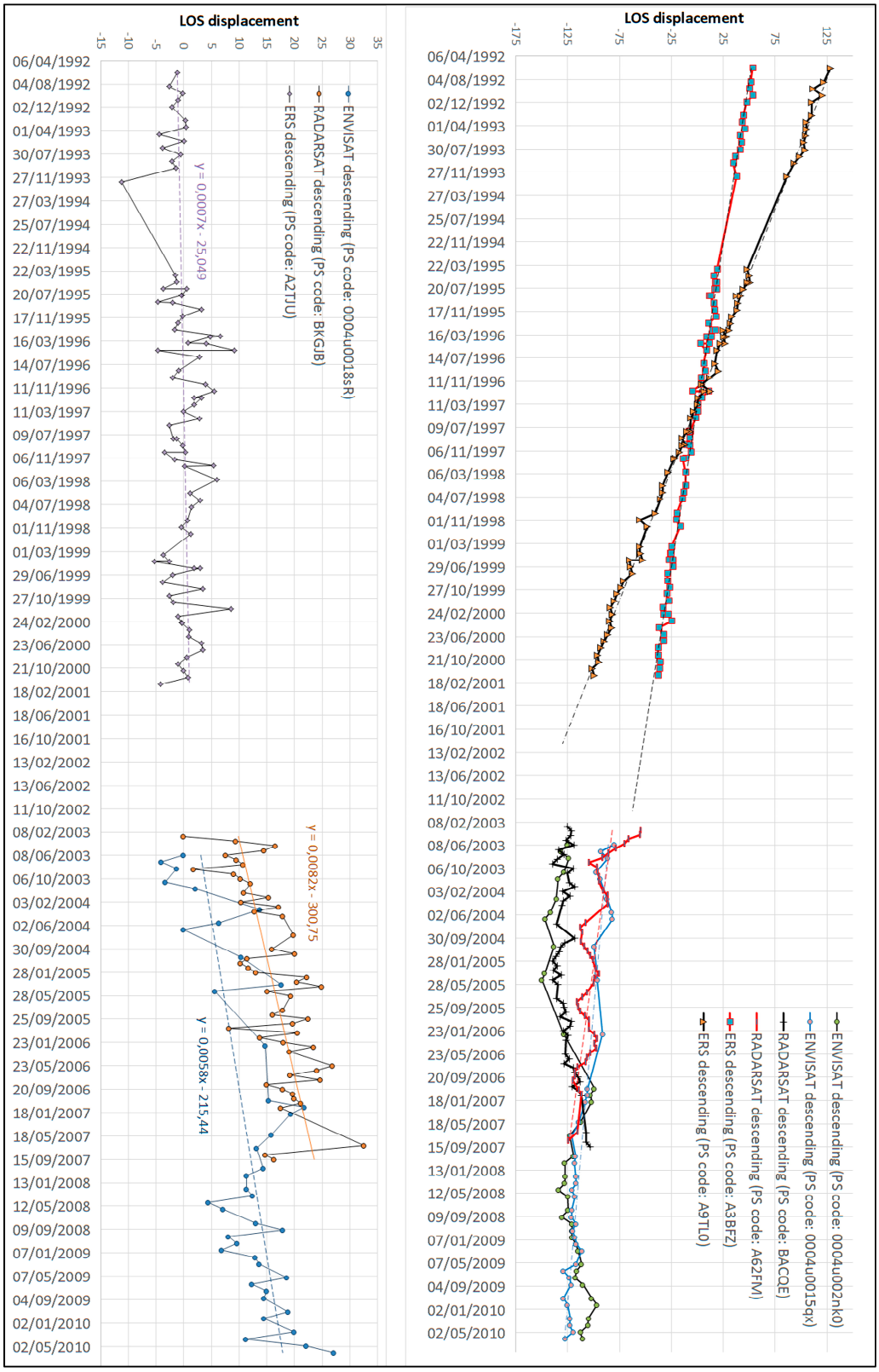

(**a**) (**b**)

Figure 8. Time series of exemplicative PS located in the study area: a) comparison between time series of PSs located near San Tammaro in uplifting sector (PS codes: A2TJU, BKGJB, 0004u0018sR); b) comparison between time series of PSs located near Grazzanise in subsiding sectors (PS codes: A3BFZ, A62FM, 0004u0015qx) and PS in Phlegrean Fields area (PS codes: A9TL0, BACQE, 0004u002nk0).

Preprints (www.preprints.org) | NOT PEER-REVIEWED | Posted: 16 November 2017 doi:10.20944/preprints201711.0112.v1

Peer-reviewed version available at Geosciences 2018, 8, 8; doi:10.3390/geosciences8010008

The overlay of the main trends of subsidence with a geological map of the study area (Fig. 9)suggests, instead, that vertical ground deformation could be partly controlled by the lithology and stratigraphic architecture of geological units forming the subsurface of the alluvial plain.

The occurrence of several tens of meters thick Holocene alluvial deposits in the axial zone of the Volturno plain, between the cities of Capua, Grazzanise, Cancello Arnone and Castelvolturno, and subordinately at the Volturno River mouth, suggests that the high subsidence values (from – 30 mm to – 418 mm) recorded in this area may be affected by the nature of the subsurface geological units (Fig. 9). Particularly, the highest subsidence values (lower than – 170 mm) detected in the vicinity of Grazzanise and Castelvolturno may be correlated with the occurrence of thick peat layers in the subsurface. These layers are characterized by successions of organic clays, peat layers and alluvial brackish deposits (Coastal plain, Swamp and Lagoon deposits) (Fig. 10) that are easily compressible by lithostatic load [37, 62, 63]. They were formed as a result of the accumulation of flood plain sediments by the Volturno river during the transition between the late phase (Early-Middle Holocene) of the post-glacial marine transgression and the Late Holocene progradation of the Volturno delta system [62, 63]. In these areas, subsidence has been ostensibly driven by enhanced sediment compaction following the rapid progradation of the coastal environments during the Holocene [37, 63].

This peculiar geological setting, also common to other major deltas of the Mediterranean region and Asia, can be recognized in the stratigraphic section of Fig. 10. Recent studies [7, 83, 84, 85, 86, 87] have suggested that natural compaction of alluvial/coastal plain deposits may cause subsidence of several millimeter/year, especially in organic-rich deposits, although still poor information exists on the magnitude of the expected compaction rates.

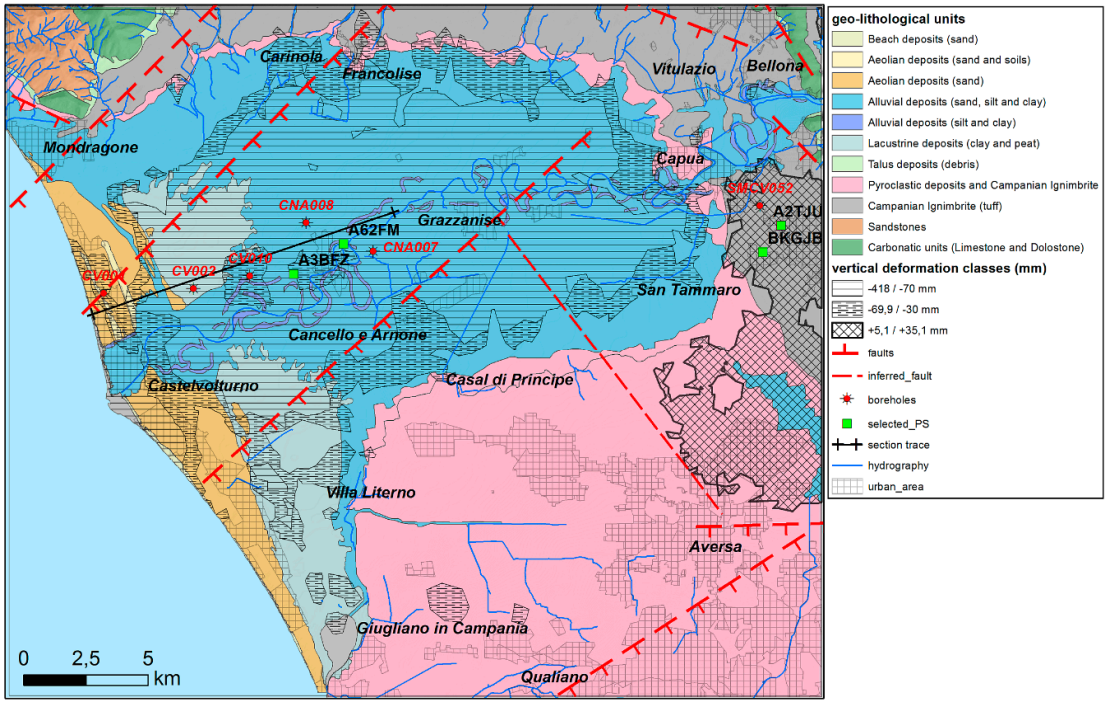

Figure 9. Correlation between cumulated amount of vertical ground displacement classes, mapped in classes with wide thresholds to better highlight the main trends, and geology maps.

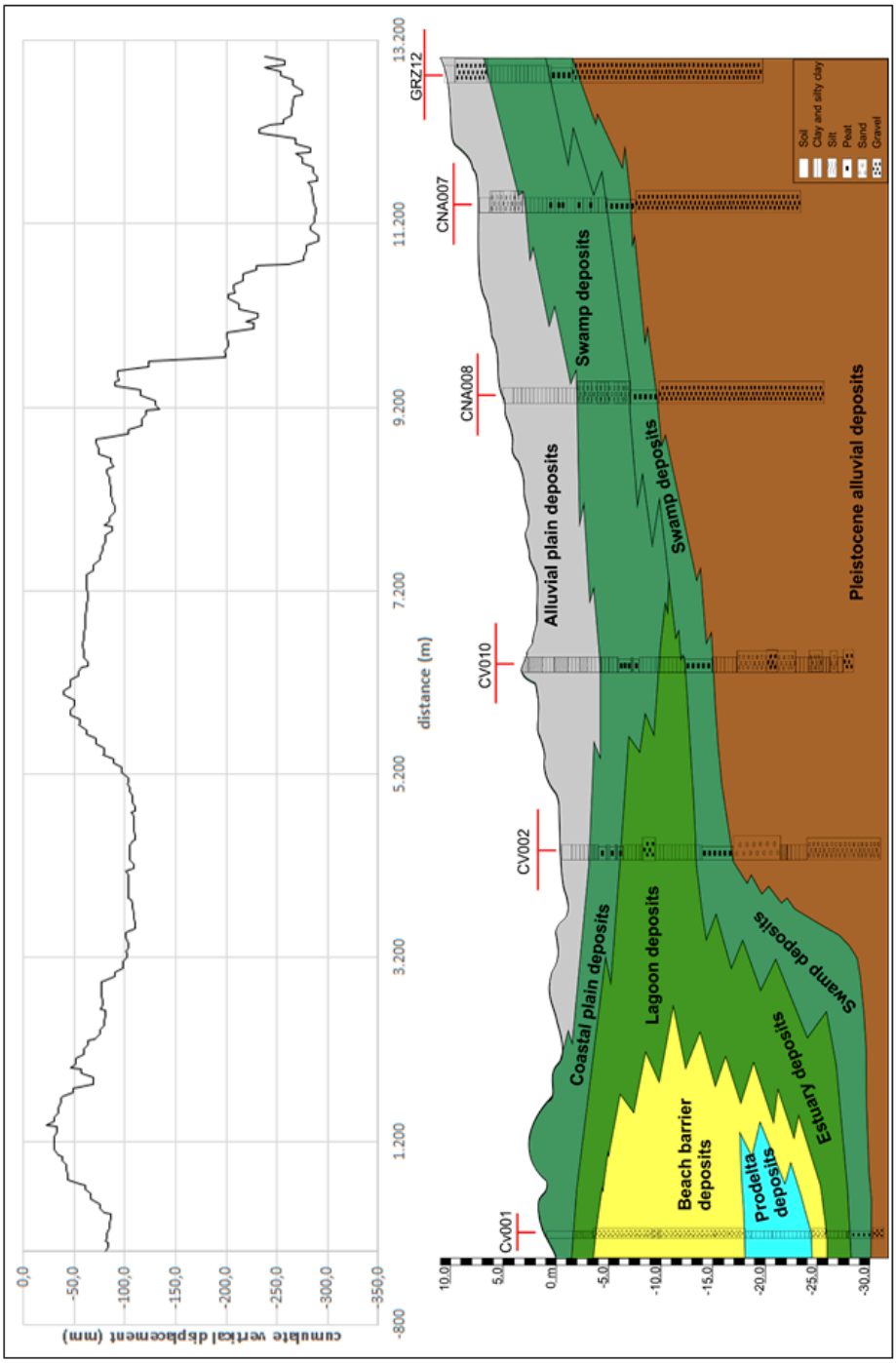

Figure 10. Correlation between stratigraphy and vertical velocity of displacement detected by SAR data.

The enhancement of the natural subsidence process may result from the uncontrolled groundwater exploitation, especially in the urban areas of the inner sector of the plain and along the coast, where the highest values of subsidence can be observed (Fig. 5).

In the north-eastern sector of the study area, the Campanian Ignimbrite tuff, locally covered by thin pyroclastic layers or alluvial and colluvial deposits, represents the main relative bedrock (Fig. 9 and 11). These tuffaceous units are formed mainly by consolidated rocky materials, and are substantially unaffected by the compaction processes due to secondary consolidation occurring under the lithostatic load of thick alluvial deposits. This geological setting may explain why

Preprints (www.preprints.org) | NOT PEER-REVIEWED | Posted: 16 November 2017 doi:10.20944/preprints201711.0112.v1

Peer-reviewed version available at Geosciences 2018, 8, 8; doi:10.3390/geosciences8010008

subsidence processes do not affect areas where the Campanian Ignimbrite and associated volcaniclastic covers units occur at shallow depth beneath the ground surface.

Unlike the central area of the Volturno delta Plain, the eastern sector of the study area is characterized by a slight uplift (values from + 10 to + 40 mm during 1992-2000) (Fig. 9). Uplift appears to be continuous during the analyzed time intervals (1992-2000, 2003-2007 and 2003-2010) (Fig. 5). When analyzing displacement time series (Fig. 8a), we may observe a change in uplift rates between the two decades of observation, as already detected from maps of Fig. 5. Minor oscillations possibly related to annual episodes of rainfall and groundwater variations can be also identified. Actually, the uplifting sector is bounded to the south by the lateral termination of an E-W trending normal fault, known as the "Cancello fault" [51]. This tectonic element is located south of Marcianise (Fig. 6), and has a vertical slip rate of ca. 1 mm/yr from 130 ky to the present day, estimated on the basis of morpho-tectonic analysis [51]. The area to the north to the fault is characterized by average uplift between 1 and 4 cm in 19 years, corresponding to a vertical rate of 0.5 to 2 mm/yr. This scenario seems to be compatible with an active tectonic uplift component controlled by the "Cancello" fault activity and its estimated vertical rates. The south-western structural boundary between uplifting and subsiding sectors is tentatively interpreted as a fault zone, located between Casal di Principe and San Tammaro (Fig. 9).

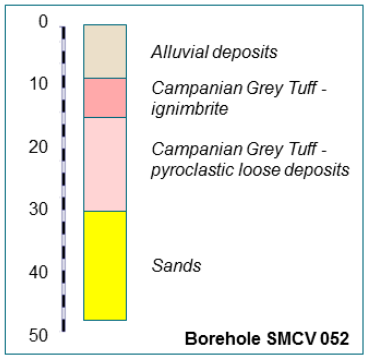

Fig. 11 – Example of a borehole stratigraphy inside the uplifting sector. For borehole location, see Fig. 9.

6. Conclusions

The analysis and interpretation of three SAR datasets of ascending and descending orbits acquired over the Campania coastal sectors during the period June 1992 – July 2010 provides new insights into the spatial variability of vertical ground deformation (subsidence/uplift) of Volturno River coastal plain. These data are in agreement with the long-term tectonic subsidence process affecting the whole Tyrrhenian margin [45, 46, 47, 48].

Ground deformation occurring in the Volturno plain resulted to be fully detectable by the SAR techniques. With reference to a period of about twenty years (1992-2010), we have documented a significant, continuous subsidence in some sectors of the alluvial and coastal plain and a moderate uplift in the eastern sector of the plain. Ground deformation patterns have been consistently imaged, even though with minor differences, by the different SAR datasets.

Integration of the three datasets has provided advantages with respect to the use of a single dataset:

1. By averaging and cumulating the different dataset we have minimized the contributions resulting from the different acquisition geometry (LOS angles) and SAR technique processing (PS-InSAR and PSP) of ERS-1/2 – ENVISAT satellites with respect to the RADARSAT satellite;
2. By using multi-annual time series with different duration we have encompassed a longer time period of observation, so that the final results of cumulated amount of vertical ground displacement is less affected by local and short-term changes.

Peer-reviewed version available at Geosciences 2018, 8, 8; doi:10.3390/geosciences8010008

According to our interpretation, subsidence of the Volturno plain can be regarded as a natural process, mainly due to the compaction under lithostatic load of the alluvial/transitional sediments fill. The magnitude of recorded subsidence was found to be greater where peat layers occur in the subsoil. Conversely, anthropic influence (e-g- water pumping, urbanization) can be only considered as an additional factor that may locally enhance subsidence processes. The detected uplift involving the eastern part of the study area is likely compatible with the tectonic activity already documented in the area [51].

The results of this study confirm the fundamental importance of using SAR data for a full understanding of rates and patterns of the recent ground deformation over coastal plain regions within tectonically active continental margins. They also provide a valuable tool for a correct territorial management strategy addressed to coastal risk mitigation.

Conflicts of Interest: We thank three anonymous reviewers for their comments and suggestions that helped us to improve earlier versions of the manuscript. The authors declare no conflicts of interest. Founding sponsors had no role in the design of the study; in the collection, analyses, or interpretation of data; in the writing of the manuscript, and in the decision to publish the results.

References

1. Frihy O.E., El Sayed E.E., Deabes E.A., Gamai I.H. (2010). Shelf sediments of Alexandria region, Egypt: Explorations and evaluation of offshore sand sources for beach nourishment and transport dispersion. Marine Georesources and Geotechnology 28, 250-274.
2. Teatini P., Tosi L., Strozzi T. (2011). Quantitative evidence that compaction of Holocene sediments drives the present land subsidence of the Po Delta, Italy. J. Geophys. Res, 116.
3. Teatini P., Tosi L., Strozzi T., Carbognin L., Cecconi G., Rosselli R., Libardo S. (2012). Resolving land subsidence within the Venice Lagoon by persistent scatterer SAR interferometry. Phys. Chem. Earth, 40-41, 72-79.
4. Higgins S.A. (2015). Review: Advances in delta-subsidence research using satellite methods. Hydrogeol. J. 24, 587–600.
5. Warrick R. A., Provost C. L., Meier M. F, Oerlemans J., Woodworth P. L. 1996. Changes in sea level, Climate Change. In: The Science of Climate Change, 359-405.
6. Xie X., Heller P. 2006. Plate tectonics and basin subsidence history. Geological Society of America Bulletin, 121 (1–2), 55–64.
7. Long, A. J.,Waller, M. P. & Stupples, P. 2005. Driving mechanisms of coastal change: Peat compaction and the destruction of late Holocene coastal wetlands. Mar. Geol. 225, 63–84.
8. Poland JF, Davis GH. 1969. Land subsidence due to withdrawal of fluids. Rev Eng Geol. 2, 187–269.
9. Galloway DL, Burbey T.J., 2011. Review: regional land subsidence accompanying groundwater extraction. Hydrogeol. J., 19:1459–86.
10. Burgmann, R., P.A. Rosen, E.J. Fielding. 2000. Synthetic aperture radar interferometry to measure Earth's surface topography and its deformation. Annual Review of Earth and Planetary Sciences 28: 169–209.
11. Strozzi, T., U. Wegmüller, L. Tosi, G. Bitelli, V. Spreckels. 2001. Land subsidence monitoring with differential SAR interferometry. Photogrammetric Engineering and Remote Sensing 67 (11), 1261–1270.
12. Herrera, G., Fernández J.A., Tomás R., Cooksley Mulas G.J. 2009. Advanced interpretation of subsidence in Murcia (SE Spain) using A-DInSAR data-modelling and validation. Natural Hazards and Earth System Science 9, 647–661.
13. Terranova C., Iuliano S., Matano F., Nardo S., Piscitelli E., Cascone E., D'Argenio F., Gelli L., Alfinito M., Luongo G., 2009. The TELLUS Project: a satellite-based slow-moving landslides monitoring system in the urban areas of Campania Region. Rend. online Soc. Geol. Ital. 8, 148-151.
14. Hanseen, R. F. 2001. Radar Interferometry, Data Interpretation and Error Analysis. Kluwer Academic Publishers. ISBN 978-0792369455
15. Hooper, A., H. Zebker, P. Segall, B. Kampes. 2004. A new method for measuring deformation on volcanoes and other natural terrains using InSAR persistent scatterers." Geophysical Research Letters 31 (L23611): 1-5. doi: 10.1029/2004GL021737;
16. Vilardo G., Ventura G., Terranova C., Matano F., Nardò S. 2009. Ground deformation due to tectonic, hydrothermal, gravity, hydrogeological and anthropic processes in the Campania Region (Southern Italy)

534 from Permanent Scatterers Synthetic Aperture Radar Interferometry. Remote Sensing of Environment 113,
535 197–212. doi:10.1016/j.rse.2008.09.007
536 17. Tofani V., Raspini F., Catani F., Casagli N., 2013. Persistent Scatterer Interferometry (PSI) Technique for
537 Landslide Characterization and Monitoring. Remote Sens., 5, 1045-1065
538 18. Gabriel, A.K.; Goldstein, R.M.; Zebker, H.A. Mapping small elevation changes over large areas: Differential
539 radar interferometry. J. Geophys. Res. 1989, 94, 9183–9191.
540 19. Costantini M., Falco S., Malvarosa F., Minati F., Trillo F., Vecchioli F. (2014) Persistent Scatterer Pair
541 Interferometry: Approach and Application to COSMO-SkyMed SAR Data. IEEE Journal of Selected Topics
542 in Applied Earth Observations and Remote Sensing, 7, 7, 2869-2879.
543 20. Regione Campania – Settore Difesa del Suolo (2009b). Progetto TELLUS WebGIS (PSInSAR). Accessed
544 September 2017 at http://webgis.difesa.suolo.regione.campania.it:8080/psinsar/map.phtml
545 21. Regione Campania – Settore Difesa del Suolo (2009a) – Progetto TELLUS web page. Accessed September
546 2017 at http://www.difesa.suolo.regione.campania.it/content/category/4/64/92/
547 22. Terranova C., Iuliano S., Matano F., Nardò S., Piscitelli E. (2009) – Relazione finale del Progetto TELLUS,
548 79 pp., Napoli, February 2009. PODIS Project of the Italian Ministry of Environment and of Protection of
549 Territory and Sea – Campania Region. Accessed September 2017 at
550 http://www.difesa.suolo.regione.campania.it/content/category/4/64/92/
551 23. EPRS-E (2015) - Not-Ordinary Plan of Environmental Remote Sensing web page. National Geoportal (NG)
552 of the Italian Ministry of Environment and of Protection of Territory and Sea. Accessed September 2017 at
553 http://www.pcn.minambiente.it/GN/en/projects/not-ordinary-plan-of-remote-sensing
554 24. EPRS-E (2015) - Not-Ordinary Plan of Environmental Remote Sensing; ENVISAT ascending e ENVISAT
555 descending interferometric products. National Geoportal (NG) of the Italian Ministry of Environment and
556 of Protection of Territory and Sea. Accessed September 2017 at http://www.pcn.minambiente.it/viewer/
557 25. IREA-CNR (2017) – InSAR WebGIS. Napoli study area. ENVISAT dataset.
558 http://webgis.irea.cnr.it/webgis.html
559 26. Trasatti, E., F. Casu, C. Giunchi, S. Pepe, G. Solaro, S. Tagliaventi, P. Berardino, M. Manzo, A. Pepe, G.P.
560 Ricciardi, E. Sansosti, P. Tizzani, G. Zeni, R. Lanari. 2008. "The 2004-2006 uplift episode at Campi Flegrei
561 caldera (Italy): Constraints from SBAS-DInSAR ENVISAT data and Bayesian source inference".
562 Geophysical Research Letters 35 (L073078): 1-6. doi:10.1029/2007GL033091
563 27. Ferretti A., Prati C., Rocca F. (2001). Permanent Scatterers in SAR Interferometry. IEEE Transactions on
564 Geoscience and Remote Sensing, vol. 39, N. 1, 8-20.
565 28. Costantini, M., S. Falco, F. Malvarosa, F. Minati. 2008. "A new method for identification and analysis of
566 persistent scatterers in series of SAR images." In Proceedings of the 2008 IEEE International Geoscience
567 and Remote Sensing Symposium (IGARSS), Boston MA, USA, 7-11 July, 449–452. doi:
568 10.1109/IGARSS.2009.5417918
569 29. Costantini, M., S. Falco, F. Malvarosa, F. Minati, F. Trillo. 2009. "Method of Persistent Scatterer Pairs (PSP)
570 and high resolution SAR interferometry." In Proceedings of the 2009 IEEE International Geoscience and
571 Remote Sensing Symposium (IGARSS), Cape Town, July 12-17, 3: 904–907. doi:
572 10.1109/IGARSS.2009.5417918
573 30. Berardino, P., G. Fornaro, R. Lanari, E. Sansosti. 2002. "A new algorithm for surface deformation
574 monitoring based on small baseline differential SAR interferograms." IEEE Transactions on Geosciences
575 and Remote Sensing 40: 2375–2383. doi: 10.1109/TGRS.2002.803792
576 31. Lanari, R.; Mora, O.; Manunta, M.; Mallorqui`, J.J.; Berardino, P.; Sansosti, E. A small baseline approach for
577 investigating deformation on full resolution differential SAR interferograms. IEEE Trans. Geosci. Remote
578 Sens. 2004, 42, 1377–1386.
579 32. Lanari, R., F. Casu, M. Manzo, G. Zeni, P. Berardino, M. Manunta. 2007. "An overview of the Small Baseline
580 subset algorithm: A DInSAR technique for surface deformation analysis." Pure and Applied Geophysics
581 164: 637–661. doi: 10.1007/s00024-007-0192-9
582 33. Vilardo, G., R. Isaia, G. Ventura, P. De Martino, C. Terranova. 2010. "InSAR Permanent Scatterer analysis
583 reveals fault re-activation during inflation and deflation episodes at Campi Flegrei caldera." Remote
584 Sensing of Environment 114: 2373–2383. doi: 10.1016/j.rse.2010.05.014
585 34. Iuliano S., Matano F., Caccavale M. & Sacchi M. 2015. Annual rates of ground deformation (1993–2010) at
586 Campi Flegrei, Italy, revealed by Persistent Scatterer Pair (PSP) – SAR interferometry. Int J Remote Sens
587 36, (24), 6160–6191.

35. Terranova, C., Ventura, G., Vilardo, G., 2015. Multiple causes of ground deformation in the Napoli metropolitan area (Italy) from integrated Persistent Scatterers Din-SAR, geological, hydrological, and urban infrastructure data. Earth Sci. Rev. 146, 105–119.
36. Peduto D., Cascini L., Arena L., Ferlisi S., Fornaro G., Reale D. (2015) A general framework and related procedures for multiscale analyses of DInSAR data in subsiding urban areas. ISPRS Journal of Photogrammetry and Remote Sensing, 105, 186–210.
37. Aucelli, C.P.P., Di Paola G., Incontri P., Rizzo A., Vilardo G., Benassai G., Buonocore B., Pappone G., 2016. Coastal inundation risk assessment due to subsidence and sea level rise in a Mediterranean alluvial plain (Volturno coastal plain e southern Italy), Estuarine, Coastal and Shelf Science (2016), http://dx.doi.org/10.1016/j.ecss.2016.06.017
38. Di Paola G., Alberico I., Aucelli P.P.C., Matano F., Rizzo A., Vilardo G. 2017 Coastal subsidence detected by Synthetic Aperture Radar interferometry and its effects coupled with future sea-level rise: the case of the Sele Plain (Southern Italy). J Flood Risk Management, DOI: 10.1111/jfr3.12308
39. Cocco, E., Crimaco, L., de Magistris, M.A., 1992. Dinamica ed evoluzione del litorale campano-laziale: variazioni della linea di riva dall'epoca romana ad oggi nel tratto compreso tra la foce del Volturno e Torre S. Atti 10° Congresso AIOL, Limato (Mondragone), 543-555.
40. Donadio, C., Vigliotti, M., Valente, R., Stanislao, C., Ivaldi, R., Ruberti, D. (2017) - Anthropic vs. natural shoreline changes along the northern Campania coast, Italy. J. Coast. Cons., DOI: 10.1007/s11852-017-0563-z
41. Ruberti D., Vigliotti M., Di Mauro A., Chieffi R., Di Natale M. (2017) - Human influence over 150 years of coastal evolution in the Volturno delta system (southern Italy). Journal of Coastal Conservation, 10pp. DOI: 10.1007/s11852-017-0557-x
42. Ruberti, D., Vigliotti, M. (2017) - Land use and landscape pattern changes driven by land reclamation in a coastal area. The case of Volturno delta plain, Campania Region, southern Italy. Environmental Earth Sciences,76, 694, doi 10.1007/s12665-017-7022-xDO
43. ENEA (2008). Analisi di specifiche situazioni di degrado della qualità delle acque in Campania, in riferimento ai casi che maggiormente incidono negativamente sulle aree costiere. Roma: ENEA, Sezione Protezione-Idrogeologica.
44. Riccio T. (2016) - Analysis of subsidence in Campania Plain. Unpublished Ph.D. Thesys in Innovative Physics Methodologies For Environmental Research, cycle XXVIII, Department Of Mathematics And Physics, University of Campania "L. Vanvitelli"; pp. 67.
45. Patacca E., Sartori R., Scandone P. (1990) - Tyrrhenian basin and Apenninic arcs: kinematic relations since late Tortonian times. Mem. Soc. geol. Ital., 45, 425-451.
46. Oldow J.S., D'Argenio B., Ferranti L., Pappone G., Marsella E., Sacchi M., (1993). Large-scale ongitudinal extension in the southern Apennines contractional belt, Italy. Geology 21, 1123-1126.
47. Ferranti L., Oldow J.S., Sacchi M., (1996). Pre-Quaternary orogen-parallel extension in the Southern Apennine belt, Italy. Tectonophysics 260, 325–347.
48. Casciello E., Cesarano M., Pappone G., (2006). Extensional detachment faulting on the Tyrrhenian margin of the southern Apennines contractional belt (Italy). Journal of the Geological Society of London 163, 617–629.
49. Di Nocera S., Matano F., Pescatore T., Pinto F. & Torre M. Geological characteristics of the external sector of the Campania-Lucania Apennines in the CARG maps. Rend Online Soc Geol Ital 2011, 12, 39–43.
50. Matano F., Critelli S., Barone M., Muto F. & Di Nocera S. Stratigraphic and provenance evolution of the Southern Apennines foreland basin system during the Middle Miocene to Pliocene (Irpinia-Sannio successions, Italy). Mar Pet Geol 2014, 57, 652–670.
51. Cinque A, Ascione A, Caiazzo C (2000) Distribuzione spazio-temporale e caratterizzazione della fagliazione quaternaria in Appennino meridionale. In: Galadini F, Meletti C, Rebez A (ed) Le ricerche del GNDT nel campo della pericolosità sismica 1996-1999. Roma, Italy, pp 203-218.
52. Mariani M., Prato R (1988) I bacini neogenici costieri del margine tirrenico: approccio sismico-stratigrafico. Memorie della Società Geologica Italiana, 41, 519–531.
53. Milia A and Torrente MM (2003) Late Quaternary volcanism and transtensional tectonics in the Naples Bay, Campanian continental margin, Italy. Miner. Petrol. 79:49-65.
54. Milia A, Torrente MM, Massa B, Iannace P (2013) Progressive changes in rifting directions in the Campania margin (Italy): new constrains for the Tyrrhenian Sea opening. Glob. Planet. Change 109:3-17.

55. Ortolani, F. and F. Aprile (1978). Nuovi dati sulla struttura profonda della Piana Campana a sud-est del fiume Volturno, B. Soc. Geol. Ital., 97, 591-608.
56. Scandone R., Bellucci F., Lirer L., Rolandi G., (1991). The structure of the Campanian Plain and the activity of the Neapolitain volcanoes (Italy). Journal of Volcanology and Geothermal Research 48, 1–31.
57. Barberi F., Innocenti F., Lirer L., Munno R., Pescatore T., Santacroce R., (1978). The Campanian Ignimbrite: a major prehistoric eruption in the Neapolitan area (Italy). Bulletin of Volcanology 41, 1–22.
58. Di Girolamo P., Ghiara M.R., Lirer L., Munno R., Rolandi G., Stanzione D. (1984). Vulcanologia e Petrologia dei Campi Flegrei. Boll. Soc. Geol. 103, 349-413.
59. Deino, A.L., Southon, I., Terrasi, F., Campajola, L., Orsi, G., 1994. ^{14}C and $^{40}Ar/^{39}Ar$ dating of the campanian Ignimbrite. Phlegrean Fields, Italy. Abstract, ICOG-8. Berkeley. CA 3, 633.
60. De Vivo B., Rolandi G., Gans P.B., Calvert A., Bohrson W.A., Spera F.J., Belkin H.E. (2001). New constraints on the piroclastic eruptive history of the Campanian volcanic plain (Italy). Mineral Petrology 73, 47-65.
61. Deino, A.L., G. Orsi, S. de Vita, M. Piochi, 2004. The age of the Neapolitan Yellow Tuff caldera-forming eruption (Campi Flegrei caldera, Italy) assessed by Ar-40/Ar-39 dating method. Journal of Volcanology and Geothermal Research, 133, 157–170. doi: 10.1016/S0377-0273(03)00396-2
62. Amorosi A., Pacifico A., Rossi V., Ruberti D., (2012) - Late Quaternary incision and deposition in an active volcanic setting: the Volturno valley fill, southern Italy. Sedimentary Geology 282, 307-320.
63. Sacchi M., Molisso F., Pacifico A., Vigliotti M., Sabbarese C., Ruberti D., (2014). Late-Holocene to recent evolution of Lake Patria, South Italy: an example of a coastal lagoon within a Mediterranean delta system. Glob. Planet. Change 117, 9-27.
64. Pappone, G., Alberico, I., Amato, V., Aucelli, P.P.C., Di Paola, G., 2011. Recent evolution and the present-day conditions of the Campanian Coastal plains (South Italy): the case history of the Sele River Coastal plain. WIT Trans. Ecol. Environ. 149, 15-27. http://dx.doi.org/10.2495/CP110021.
65. Scorpio, V., Aucelli, P.P., Giano, S.I., Pisano, L., Robustelli, G., Rosskopf, C.M., Schiattarella, M., 2015. River channel adjustments in Southern Italy over the past 150 years and implications for channel recovery. Geomorphology 251, 77-90.
66. Barra, D., Romano, P., Santo, A., Campaiola, L., Roca, V., Tuniz, C., 1996. The Versilian transgression in the Volturno river plain (Campania, Southern Italy): Palaeoenvironmental history and chronological data. Il Quat. 9 (2), 445-458.
67. Amorosi, A., Molisso, F., Pacifico, A., Rossi, V., Ruberti, D., Sacchi, M., Vigliotti, M., 2013. The Holocene evolution of the Volturno River coastal plain (southern Italy). J. Mediterr. Earth Sci. 5 (Special Issue 7-1), 7-11.
68. Romano, P., Santo, A., Voltaggio, M., 1994. L'evoluzione morfologica della pianura del fiume Volturno (Campania) durante il tardo Quaternario. Il Quat. 7 (1), 41-56.
69. Lambeck, K., Antonioli, F., Anzidei, M., Ferranti, L., Leoni, G., Scicchitano, G., Silenzi, S. (2011) - Sea level change along the Italian coast during the Holocene and projections for the future. Quaternary International 232: 250-257.
70. Putignano M.L., Ruberti D., Tescione M. and Vigliotti M. (2007) - Evoluzione recente di un territorio di pianura a forte sviluppo urbano: la Piana Campana nell'area di Caserta. Boll. Soc. Geol. It., 126, 11-24.
71. Lu, Z., Kwoun, O., & Rykus, R. (2007). Interferometric syntetic aperture radar (InSAR): Its past, present and future. Photogrammetric Engineering & Remote Sensing, 73(3), 217–221.
72. Rott, H. (2009). Advances in interferometric synthetic aperture radar (InSAR) in earth system science. Progress in Physical Geography, 33(6), 769–791, doi: 10.1177/0309133309350263.
73. Vasco, D. W., Rucci, A., Ferretti, A., Novali, F., Bissell, R. C., Ringrose, P. S., Mathieson, A. S., & Wright, I. W. (2010). Satellite-based measurements of surface deformation reveal fluid flow associated with the geological storage of carbon dioxide. Geophys. Res. Lett., 37, L03303, doi:10.1029/2009GL041544.
74. Colesanti, C., Locatelli, R., Novali, F., 2002. Ground deformation monitoring exploiting SAR permanent scatterers. IEEE IGARSS 2, 1219-1221.
75. Colesanti, C., Ferretti, A., Locatelli, R., Novali, F., Savio, G., 2003. Permanent Scatterers: precision assessment and multi-platform analysis. IEEE IGARSS 2, 1193-1195.
76. Colesanti, C.,Wasowski, J., 2006. Investigating landslides with spaceborne synthetic aperture radar (SAR) interferometry. Eng. Geol. 88, 173-199.

694 77. Ferretti, A., G. Savio, R. Barzaghi, A. Borghi, S. Musazzi, F. Novali, C. Prati, F. Rocca. 2007. "Submillimeter
695 accuracy of InSAR time series: Experimental validation." IEEE Transactions on Geoscience and Remote
696 Sensing 45 (5): 1142–1153. doi: 10.1109/TGRS.2007.894440
697 78. Massironi, M., Zampieri, D., Bianchi, M., Schiavo, A., & Franceschini, A. (2009). Use of PSInSAR™ data to
698 infer active tectonics: Clues on the differential uplift across the Giudicarie belt (Central-Eastern Alps, Italy).
699 Tectonophysics, 476, 297–303, doi:10.1016/j.tecto.2009.05.025.
700 79. Franke, R., 1982. Scattered data interpolation: test of some methods. Math. Comput. 33, 181-200.
701 80. Mueller, T.G., Pusuluri, N.B., Mathias, K.K., Cornelius, P.L., Barnhisel, R.I., Shearer, S.A., 2004. Map quality
702 for ordinary kriging and inverse distance weighted interpolation. Soil Sci. Soc. Am. J. 68, 2042-2047.
703 81. Lundgren, P., F. Casu, M. Manzo, A. Pepe, P. Berardino, E. Sansosti, R. Lanari. 2004. "Gravity and magma
704 induced spreading of Mount Etna volcano revealed by satellite radar interferometry." Geophysical
705 Research Letters 31(L04602). doi: 10.1029/2003GL018736
706 82. Manzo, M., Ricciardi, G. P., Casu, F., Ventura, G., Zeni, G., Borgström, S., Berardino, P., Del Gaudio, C., &
707 Lanari, R. (2006). Surface deformation analysis in the Ischia island (Italy) based on spaceborne radar
708 interferometry. Journal of Volcanology and Geothermal Research, 151, 399–416.
709 83. Meckel T. A., Brink U. S.,Williams S. J. (2007). Sediment compaction rates and subsidence in deltaic plains:
710 numerical constraints and stratigraphic influences. Basin Research 19, 19–31.
711 84. Meckel T.A., Brink U.S.,Williams S.J. (2006) - Current subsidence rates due to compaction of Holocene
712 sediments in southern Louisiana. Geophysical Research Letters, Vol. 33, L11403.
713 85. Shi C., Zhang D., You L., Li B., Zhang Z., Zhang O. (2007). Land subsidence as a result of sediment
714 consolidation in the Yellow River Delta. J Coast Res 23(1), 173–181.
715 86. Tornqvist T.E., Wallace D.J., Storms J.E.A., Wallinga J., Van Dam R.L., Blaauw M., Derksen M.S., Klerks
716 C.J.W., Meijneken C., Snijders E.M.A. (2008) - Mississippi Delta subsidence primarily caused by compaction
717 of Holocene strata. Nature Geoscience 1, 173-176.
718 87. van Asselen, S. (2011). The contribution of peat compaction to total basin subsidence: implications for the
719 provision of accommodation space in organic-rich deltas. Basin Research 23, 239–255.